



Western Washington University
Western CEDAR

WWU Honors Program Senior Projects

WWU Graduate and Undergraduate Scholarship

Spring 2002

Geologic Modeling of Magnetic Data for Cypress Island, Washington

Ian Mynatt

Follow this and additional works at: https://cedar.wvu.edu/wwu_honors



Part of the [Geology Commons](#)

Recommended Citation

Mynatt, Ian, "Geologic Modeling of Magnetic Data for Cypress Island, Washington" (2002). *WWU Honors Program Senior Projects*. 258.

https://cedar.wvu.edu/wwu_honors/258

This Project is brought to you for free and open access by the WWU Graduate and Undergraduate Scholarship at Western CEDAR. It has been accepted for inclusion in WWU Honors Program Senior Projects by an authorized administrator of Western CEDAR. For more information, please contact westerncedar@wwu.edu.

**GEOLOGIC MODELING OF MAGNETIC DATA
FOR
CYPRESS ISLAND, WASHINGTON**

Ian Mynatt

Spring 2002



HONORS THESIS

In presenting this Honors paper in partial requirements for a bachelor's degree at Western Washington University, I agree that the library shall make its copies freely available for inspection. I further agree that extensive copying of this thesis is allowable only for scholarly purposes. It is understood that any publication of this thesis for commercial purposes or for financial gain shall not be allowed without my written permission.

Signature 

Date 11/11/02

Abstract: Cypress Island, Washington is composed of three distinct rock units separated by two major faults with east-west trending surface traces. The rock units are from south to north; an ultramafic unit with varyingly serpentinized harzburgite, a volcanic/sedimentary unit composed of basalt, numerous pelagic sediments and serpentine, and a greywacke unit. The orientations of the fault contacts at depth are not interpretable by surface data. This study compiled magnetic data from several sources to model subsurface geologic aspects of the island. Magnetic anomaly profiles were created from the data, then analyzed and modeled using the computer program *GM-SYS*. The primary goal of this study was to model the orientation of the fault separating the ultramafic unit from the volcanic/sedimentary unit. The results indicate that the fault has a high-angle south dipping orientation. Data collected also indicate unexpected large quantities of subsurface magnetic material in the volcanic/sedimentary unit. Due to the presence of small amounts of serpentine found as outcrop in this unit, these subsurface magnetic bodies are interpreted to be serpentine as well. The distribution and quantity of this serpentine suggests that the sedimentary/volcanic unit is a serpentine melange.

Introduction: Cypress Island, of the San Juan Islands, Washington, presents a near ideal location for using modeling of magnetic anomaly data to examine and describe sub-surface geologic characteristics. The island has both important structures that are not interpretable by surface data alone, and a unique arrangement of rock units of highly varied magnetic susceptibilities creating excellent magnetic anomaly profiles. These profiles present the opportunity to model and interpret the sub-surface characteristics of the island to create a more complete picture of the structures only hinted at by exposures at the surface. This study added newly collected magnetic data to a compilation of previously measured data with the purpose of modeling large-scale structures of Cypress Island.

Cypress Island lies on the eastern edge of the San Juan Islands, which are located between Vancouver Island, British Columbia, and the northern coast of Washington. The overall composition of the island is fairly simple with three distinct rock units separated by two major faults with roughly east-west surface traces (Fig. 1). However, the geometries of these faults at depth are ambiguous and preliminary fieldwork done for this study examining surface exposures found no definitive structural indication of orientation or offset for either. Previous work concurs with this finding, with McLellan (1927) and Whetten (1975) mapping both faults as south-dipping thrusts, with the dip of the northern fault "inferred". More recently, Lapen (2000) mapped only the surface traces and specified the dips and offsets of both as unknown. This uncertainty is the result of a lack of well-exposed contacts, as much of the island is covered in growth and exposed rocks are often extensively weathered.

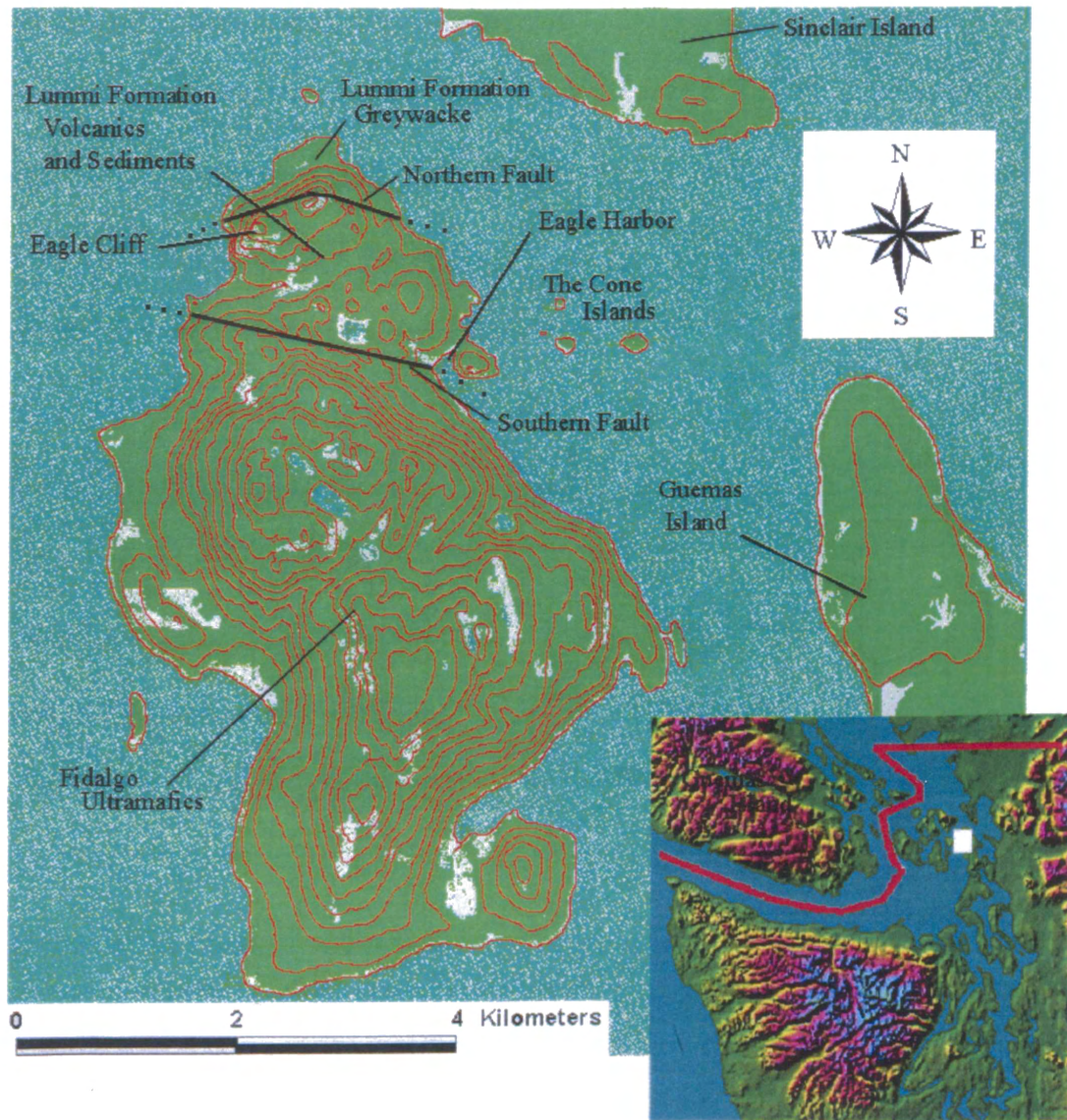


Figure 1. Map of Cypress Island showing relevant locations, including the two major faults and the rock units separated by the faults. The southern fault was modeled in this study. Fault traces are those mapped by Lapen (2000). Inset shows study location as white rectangle (modified from Sterner, 1995).

The southern fault separates highly magnetic ultramafic rocks in the southern two-thirds of the island from magnetically quiet volcanic and sedimentary rocks in the middle. These volcanics and sediments are then separated from similarly magnetically quiet greywacke to the north by the northern fault (Fig. 1). Based on this configuration

and the properties of these units, a north-south magnetic profile of the island reflects almost exclusively characteristics of the ultramafic rocks. By modeling the shape of the ultramafic unit using the large-scale aspects of such profiles, the orientation of the ultramafic-volcanic/sedimentary contact, and therefore the geometry of the southern fault at depth, can be examined. This was the primary focus of the study. While the northern fault cannot be examined in this manner, as it is a contact between relatively non-magnetic units, other implications for sub-surface configuration based on the smaller scale aspects of the data can be modeled and considered.

Although magnetic data had previously been collected for the area in general and for the island in particular, a comprehensive attempt to model the sub-surface structures of the island had not been performed. This study compiled a number of these data sources, along with collecting new data, to create and compare multiple models of the island.

Geology: Cypress Island has experienced the scrutiny of geologists for a considerable length of time. These investigations have ranged from perfunctory glances as part of larger studies to in-depth petrologic examinations of one unit of the island (Brandon et al., 1988; Raleigh, 1965). As a result of these studies, and the presence of the same rock units on Cypress as at other closely examined locations, a considerable amount is known and surmised about the geologic history of the area and the island.

Jurassic ultramafic rocks comprise the southern two-thirds of Cypress Island and correlate with the lowest part of the Fidalgo ophiolite of Brown et al. (1979) and the Fidalgo Igneous Complex of Brandon et al. (1988) (Fig. 1). They are also exposed on

several surrounding islands, including excellent outcrops on nearby Fidalgo Island (Gussey, 1978; Lapen, 2000). Serpentinization from hydrothermal alteration has occurred in varying amounts throughout the unit, causing local areas to appear from near black to slippery green. Unserpentinized areas are predominantly harzburgite with small areas of dunite (Brown et al., 1979; Lapen, 2000). These rocks have generally been interpreted to be the lowest part of an ophiolite. On Fidalgo Island they lie at the base of an essentially continuous stratigraphic column with overlying gabbro and tonalite topped by felsic volcanic sediments. Based on this sequence and chemical analysis, this complex is thought to be of island arc origin, although that interpretation is not conclusive (Brown et al., 1979). Other possibilities include that the ultramafics are the base of a regular piece of ocean crust, or the base of continental crust.

The northernmost unit of Cypress Island is a well bedded to massive greywacke cross cut by an extensive quartz vein system representing several periods of post depositional deformation. These greywackes are considered part of the Lummi Formation as identified by Vance (1975). Turbidite sequences along with other structures suggest that these rocks were deposited in a sub-marine environment (Brandon et al., 1988). The rocks on Cypress Island represent only a portion of the total unit that can be observed more completely on Lummi Island. On Lummi Island, the unit ranges from pebble conglomerate to mudstone, with greywacke as an intermediate. Also on Lummi Island, gradationally underlying these epiclastic sediments are radiolarian cherts (Carroll, 1980; Lapen, 2000). The age of this unit has been determined as late Jurassic to early Cretaceous (Carroll, 1980).

The middle section of this island is predominantly Jurassic pillow basalt, basaltic breccia and to a lesser extent greywacke. This is a marked difference from the other two units comprising the island which are both composed almost exclusively of one distinct rock type. Like the northern greywacke unit, this middle unit is classified as part of the Lummi Formation. Elsewhere, correlated Lummi Formation basalts have been defined as mid-ocean ridge basalts (MORB), or remains of ocean floor formed at a spreading center upon which oceanic sediments were deposited (Brandon et al., 1988). Excellent corresponding outcrops on nearby Lummi Island showing pillow basalts overlain by chert, argillite and greywacke are evidence for this ocean crust interpretation. The basalt of Cypress Island's middle section contains many discernable pillows and this, along with chemical analysis, implies it too is MORB (M.C. Blake, Western Wash. Univ., unpublished data, 2000). However, as mentioned, many other rock types are also present in the middle section of Cypress Island.

The most thoroughly distributed of these secondary rocks are blocks and lenses of serpentine, seen as large and small isolated outcrops throughout the basalt unit. Argillite and greywacke are also present, with one outcrop near Eagle Harbor 10's of meters long and tall (Fig. 1). Chert is also found in several locations. Through chemical analysis, it has been determined that the basalt that makes up Eagle Cliff on Cypress Island and parts of the near-by Cone Islands is not MORB, but a second, more alkalic basalt like those produced at mid-ocean hotspots (Fig 1). Basalt of this origin is referred to as ocean island basalt (OIB). Intrusives of the same chemistry as the OIB are also seen, presumably the remnants of the feeder dike of the OIB (M.C. Blake, Western Wash. Univ., unpublished data, 2000).

One possibility for the proximity of these two basalt types is that an island was made by intrusion of a hotspot through the ocean floor, placing the OIB on top of the MORB. This island and the underlying plate could then have been subducted and carried to depth under the overriding continental plate or island arc where they would have been metamorphosed (Fig. 2). This model is supported by the presence of the metamorphic minerals aragonite and lawsonite along with other blueschist facies minerals throughout both the greywacke and basalt sections of Cypress Island (although not in the ultramafics) (Carroll, 1980). These minerals are indicative of rocks subjected to conditions of significant depth but with relatively low temperatures, like those found in a subduction zone.

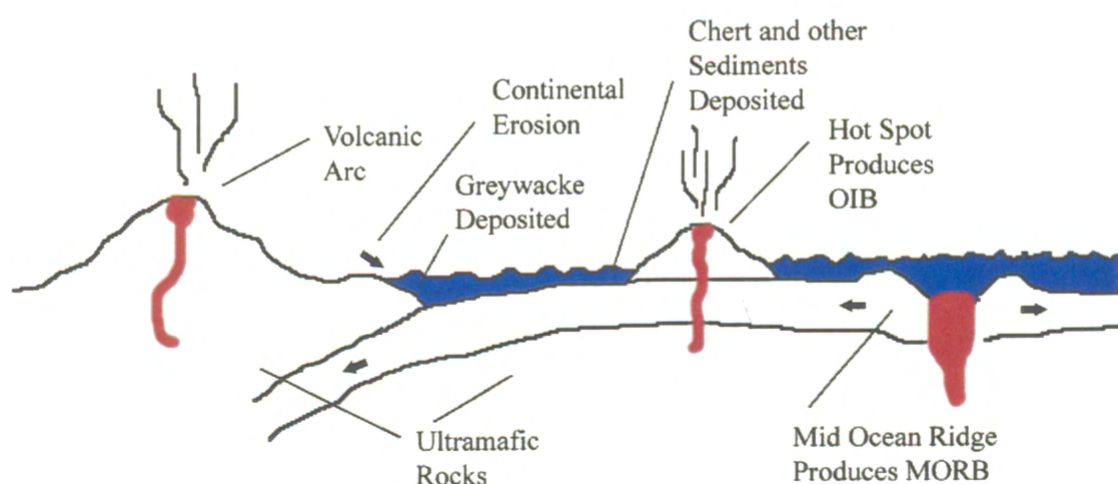


Figure 2. Possible tectonic model for rock units found on Cypress Island. Note two possible locations for the source of the ultramafic rocks.

As the island was carried to the subduction zone, chert and other pelagic sediments could accumulate. When it neared the continental margin, greywacke would then be deposited (Fig. 2). This model accounts for all of the rock types of the Lummi Formation seen on Cypress Island.

This model leaves at least two possibilities for the ultramafics. Brandon et al. (1988) suggested that the Lummi Formation was deposited on top of the Fidalgo ophiolite, including the ultramafics, during the formation of oceanic crust, making Fidalgo and Lummi part of the same terrane. More recent work has concluded that due to the differences in metamorphic grade (blueschist facies for the Lummi Formation vs. relatively unmetamorphosed Fidalgo Ophiolite), as well as structural and stratigraphic incompatibilities, these units were instead placed in proximity after being transported from different locations and are in fact separate terranes (Blake et al., 2000). A second possibility based on the model presented here is that the ultramafics were part of the overriding continental plate and were placed in contact with the Lummi Formation during subduction.

Data Collection and Preparation: The majority of the data collected and used in this study involved magnetic anomaly transects. These are collected as a series of measurements in a more or less linear path of the total magnetic field over a feature or area. The total magnetic field (also called the observed or measured field) equals the field generated by the Earth at a given point (the expected field) plus or minus any fields created by magnetic bodies large enough to affect the Earth's field at that point (the magnetic anomaly) (Fig. 3). The Earth's (expected) field is relatively constant in direction and magnitude for a given location on the Earth's surface. This field acts a vector and interacts with the anomalous fields generated by magnetic bodies in the area. These bodies' fields also act as vectors which add to or subtract from the Earth's field, creating positive and negative anomalies in the measured field.

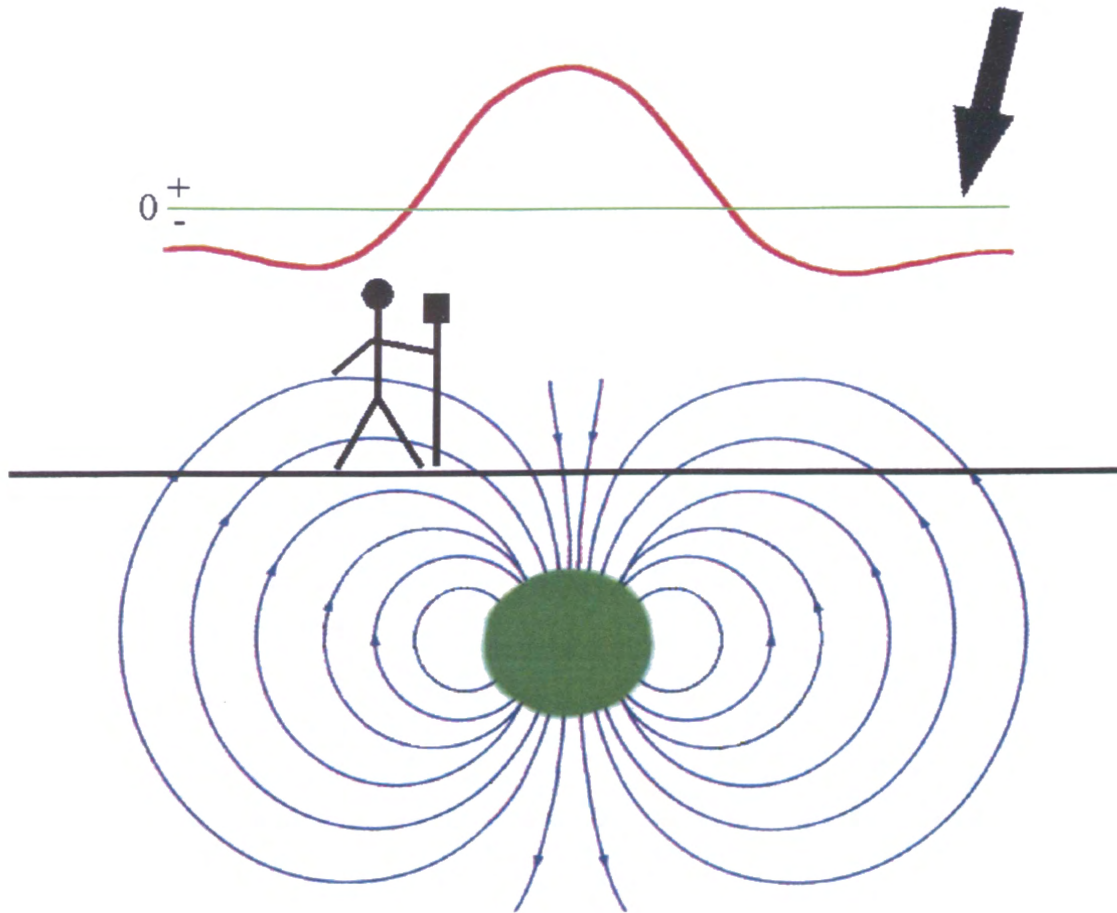


Figure 3. The vectors of the field generated by an anomalous body add to or subtract from the Earth's field at a given point creating a measurable magnetic anomaly. Where the arrows point the same direction, the anomaly is positive. Where the arrows oppose each other the anomaly is negative. Black arrow is Earth's/expected field. Blue lines are the anomalous field generated by a buried magnetic body. Red line is the total/measured field and its distance above and below the green line equals the anomaly. The person uses a magnetometer to measure the total field.

Measurements taken are of the total magnetic field, reflecting both the magnitude and direction of the Earth's field and the fields generated by any anomalous bodies. Identification of the anomalous magnetic bodies is the purpose of these measurements, and so their effect needs to be extracted from the raw total field measurements. The magnetic anomaly is the magnitude of this effect, and is calculated by subtracting the expected field at a location from the observed field. This removes the Earth's field from the measurement and leaves a positive or negative number quantifying the affect of any

anomalous magnetic bodies at that point. Combining a series of these corrected measurements in a transect creates a magnetic anomaly profile, which can then be used to interpret what the properties of the anomalous magnetic bodies may be (Fig. 4).

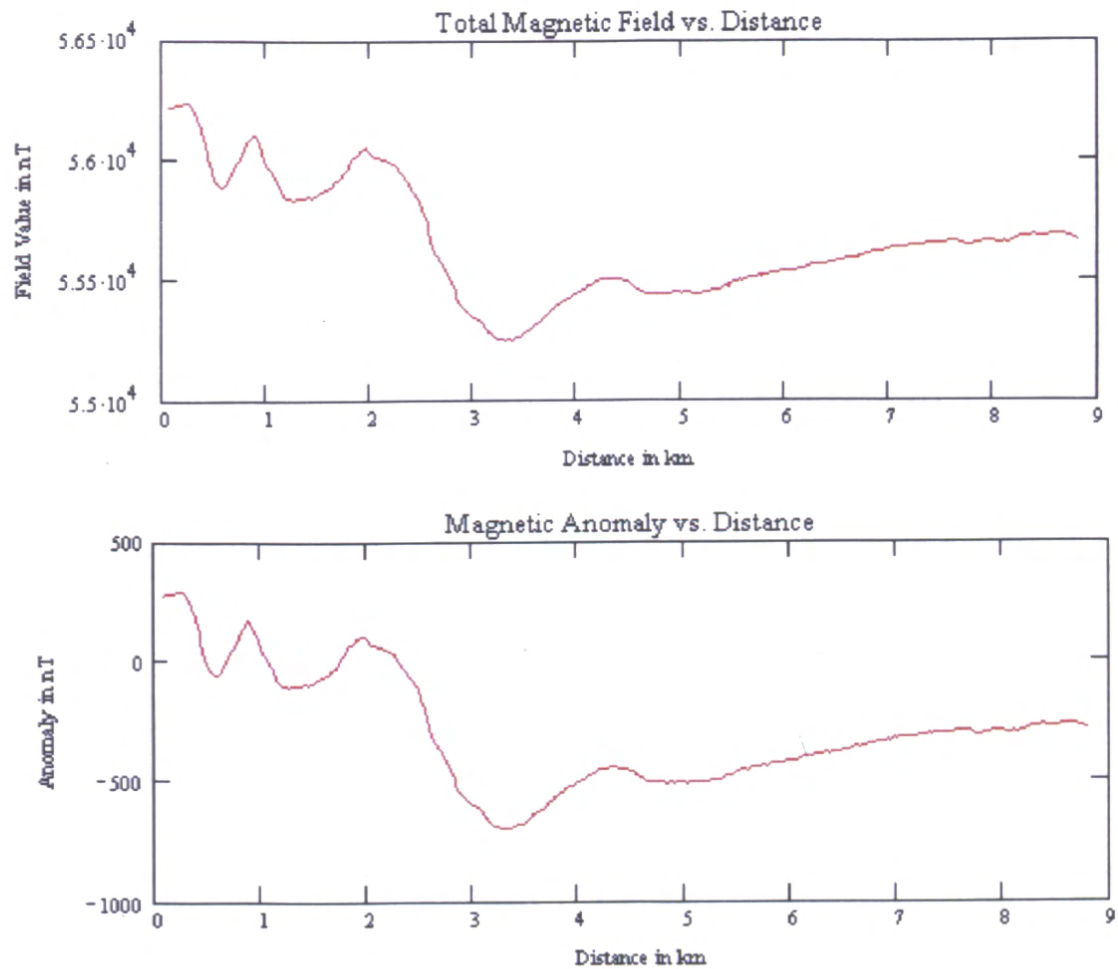


Figure 4. Upper graph shows raw observed field measurements for a water based transect of Cypress Island. Values are near those of the Earth’s magnetic field of 55,950 nT. Lower graph is anomaly values of the same transect created by subtracting the Earth’s magnetic field from the upper graph. Note minor differences in shape and positive and negative values with magnitudes less than 1000 nT. The lower graph is an anomaly profile, the data form all modeling was done with.

Magnetic data for Cypress Island were available in two forms at the beginning of this study. An air-based survey (aeromag) was conducted by Blakely et al. (1999) over most of the San Juan Islands and a significant portion of the surrounding area. These

data were taken as a grid with data points separated by 222 meters (.002°) horizontally north/south and east/west 500 meters above topography. For this study, values for two north to south transects over the island and adjacent water were extracted from this grid (Fig. 5). Water-based transects had been conducted by Engebretson (Western Wash. Univ., unpublished data, 1996) off the northeastern shore of the island. These data were much less regularly spaced and oriented, with values taken approximately every 30 meters in a roughly northwest to southeast line. Bathymetry measurements averaged around 30 meters. One transect was created from these data and used in this study (Fig. 5).

In addition to these two pre-existing data sets, a ground-based survey was conducted and used this study. The two tools used for this survey were a GPS unit and a magnetometer. The GPS unit was a *Garmin GPS III Plus*, which gives a latitude and longitude location in degrees and minutes, with minutes given to three decimal places. The magnetometer was a *Geometrics G-856 Memory-Mag Proton Precession Magnetometer*. Magnetometer readings are given in nanotesla (nT) to one decimal place. For reference, the Earth's expected magnetic field on Cypress Island is around 55,950 nT.

A north to south transect of the island was made (Fig. 5). Measurements of both location and total magnetic field were taken for approximately each hundredth of a minute distance change in latitude. This translates to measurements taken about every 20 meters along north-south line, meaning all near surface objects 10 meters and bigger would be detected by the magnetometer.

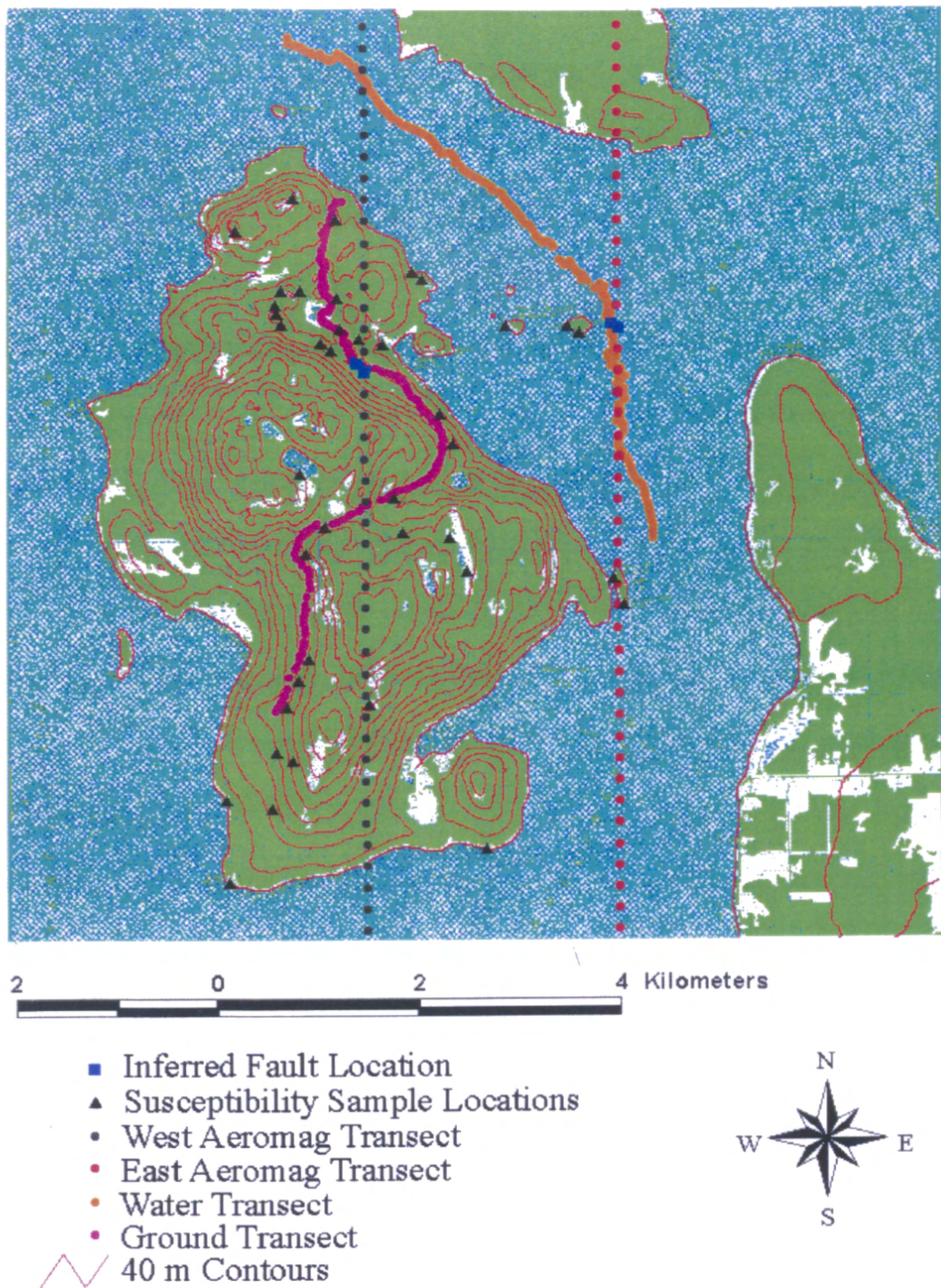


Figure 5. Locations of transects, susceptibility samples and the inferred fault locations.

All four of these transects were then converted into magnetic anomaly profiles for modeling (Appendix A). The aeromag data were already in this form, with anomaly magnitude as a function of latitude, as longitude was fixed. The water and ground based

data were in observed values. Calculating the anomaly requires the expected field value at each point. Calculations of the expected field require latitude, longitude, elevation and date to account for fluctuations of the Earth's magnetic field through space and over time. All locations and the elevation of the water based transect were known. For the ground-based transects, elevation was obtained from a digital elevation map (DEM) of the island using *ArcView* and the known latitude and longitude of each point. With this information, the program *GEOMAG* (Quinn, 2000) calculated the expected field at each data point. With the expected and observed field values known, the anomaly at each point was calculated, turning the water and ground based transects into anomaly profiles.

The final data used in this study were magnetic susceptibility values for the rocks on Cypress Island. Susceptibility is the quality of a rock that controls the relationship between the magnetic field applied to the rock and the magnetic field generated by the rock. More specifically, it is the unitless coefficient which describes the linear relationship between the applied and induced fields for a given rock ($H = kM$, where k is susceptibility, H is induced field and M is applied field). A bigger susceptibility means a larger magnitude magnetic field generated by a rock for a given applied field. In the case of Cypress Island the applied field is that generated by the Earth.

These values are important for this study for two major reasons. The first is to insure that any susceptibility values used to model the island are close to the actual values measured. The second is to confirm an assumption used to model the island, namely that the ultramafic rocks are the only rocks magnetic enough, or with high enough susceptibilities, to have contributed significantly to the measured anomalies. The basalt and greywacke are assumed to have a negligible affect on the anomaly profile as both

should have low susceptibilities. This is certainly the case for the greywacke, but basalts can and do have large susceptibilities.

Magnetic susceptibility values for rocks in the San Juan Islands are reported by Burmester (2000). This information was in database form at the Pacific Northwest Paleomagnetism Lab. While some of the samples were specified by rock type, others were only labeled by location. The locations of samples taken on Cypress Island were plotted on a map of the island using *ArcView*, thereby linking the location database to the map (Fig. 5). The database containing susceptibility values was then linked to the location database. This created a way to determine what rock types the samples were and their susceptibilities by visually observing where on the island they were taken.

The results of this inquiry supported the assumption that the ultramafic rocks are the only significant contributor to the anomalies measured on Cypress Island. The median magnetic susceptibility found from the samples for the ultramafic rocks is 0.05 in SI units and values ranged from 0.01 to 0.33. This is an order of magnitude higher than the basalt samples, which have a median of 0.008 and values from 0.002-0.06 (Appendix B). These are predominantly small enough values that the large-scale magnetic affects of these rocks can be ignored in the modeling. All values are well within the range for these rock types found by other researchers (Hunt et al., 1995).

Modeling Parameters: The modeling program used in this study was *GM-SYS* (Northwest Geophysical Associates, Inc., 1998). *GM-SYS* allows the user to design a geologic model that may have generated an observed anomaly. The program then calculates the interaction between the Earth's field and the geologic model and displays

the anomaly for that model. The observed and the modeled anomalies can then be visually inspected for correspondence and the program calculates the RMS (root mean square) misfit between the two. The model and modeled anomaly are instantaneously linked, so changes in the model immediately change the modeled anomaly. In this way the geologic model may be revised by trial and error to arrive at the smallest possible misfit between observed and modeled anomalies.

The program requires the input of several parameters. The first of these is the azimuth of the transect so that the model is oriented with respect to the Earth's field, which in all cases for this study was north-south. Next, the height of the measurements above the rocks must be specified; this is to account for the decrease in magnitude of the field generated by the rocks over distance. These values are known for all of the transects. The susceptibilities of the rocks in the model are also a variable. Values used were kept within the constraints dictated by the actual susceptibilities measured on the island, and the ultramafics and serpentine blocks were considered the only measurably magnetic rocks. Other parts of the models include air, water, basalt (representing the mixed rocks of the middle section), greywacke and unspecified "crustal rock". All of these were assigned zero magnetic susceptibility and acted as spatial fillers around the ultramafic block.

The variable with the greatest range of possibilities is the geometry of the rocks. This is strongly influenced by the field data; only rocks seen in the field were used in the model. Also, certain configurations are extremely unlikely, both based on what is seen on the island and on general knowledge of geology. The relatively simple general geometry of the contacts on Cypress Island simplified matters considerably.

A critical assumption simplifying the rock geometry was that the lowest value of the measured anomalies was located at the point where the southern (ultramafic/basalt) fault contact reached the surface. In other words, the lowest measured field value for each transect was measured directly over the fault trace (Fig. 6). This was observed in the field (Engebretson, oral communication, 2002) and was reinforced by plotting the location of several of these low values on a map. These points are aligned with the known trace of the fault (Fig. 1, 5).

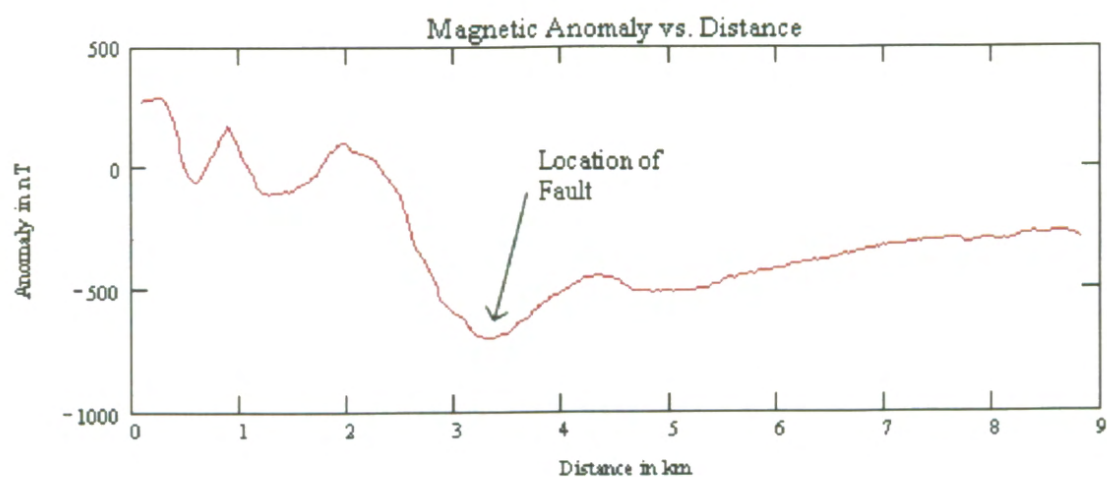


Figure 6. The lowest measured total field (and anomaly) value corresponds to the surface location of the fault. The location in latitude and longitude of these lowest measured values are plotted on figure 5, corresponding to the fault trace.

This surface trace/lowest measured value association is important as it fixes a point for the models. This reduces the possibilities for the shape and location of the fault by requiring the fault to contact the surface directly at the lowest measured field value. This meant for the fault only the dip angle and depth were orientation variables. To eliminate depth as a variable, trial models were made with the same fault orientation but with varying ultramafic block depths (e.g. 2 km vs. 20 km). This was found to have a minimal affect on the modeled anomaly, particularly after a depth of around 4 km. This

depth was chosen as a constant for all of the models as a realistic estimate of the fault depth.

Geologic Models of Cypress Island: The first step in the modeling was to ascertain the orientation of the southern, ultramafic-volcanic/sedimentary fault. This was the primary focus of the study, and it established the general geometry of the island for later, more complicated models. This was done by using the above assumptions and constants and by varying the fault dip. Susceptibility for the ultramafic unit was also adjusted for each model to acquire the best model to measured anomaly fit. Values used ranged from .012-.047 in SI.

The comparison process used was to model multiple fault dips covering the range of possibilities and examine which modeled orientation had the best fit to the measured anomalies. As the fault trace runs east to west, the only dips modeled were north, vertical and south. Five different fault orientations were used. These are north-dipping high (60°) and low (30°) angle, vertical, and south-dipping high and low angle. To check for consistency, each orientation was modeled against the same three anomaly profiles. The water transect and an aeromag transect that ran over it were chosen in order to compare the same features at different heights. Also chosen was a second aeromag transect that ran roughly over the north-south land transect (Fig. 5).

This created a total of fifteen models, or five sets of the same three transects, which were then compared. For each model, the program calculated an RMS value, which is a statistical average of the difference between the modeled and actual anomaly for all of the data points for a given transect. For this reason, differences in transect

length or number of data points are accounted for and a comparison between models can be made. This is displayed by *GM-SYS* both as a number in nanotesla (nT, magnetic field strength) and by an error line that shows the magnitude of difference at each point between the modeled and measured anomalies. For each fault orientation, the sum of the error for the three transects was calculated for comparison with the other orientations (Fig. 7, Appendix C).

After summing the error values for the three models for each fault dip orientation, the orientations were ranked with the smallest error sum being the most likely geometry. This order was south dipping high-angle with 318, vertical with 370, north dipping high-angle with 478, south dipping low-angle with 520 and north dipping low-angle with 670. Based on this, the south dipping high-angle orientation was assumed to be most likely and was then used for subsequent modeling.

The ground transect was not used in the modeling of the fault orientation. The initial purpose for this transect was to acquire near-source data to compare with the water and aeromag data in order to model the fault more accurately. However, for the north-south land transect the obvious sudden drop in the anomaly at the fault present in the air and water based transects is overwhelmed by spikes and troughs of the measured anomaly (Fig. 8). The relatively smooth anomaly curve of the water and aeromag transects which was influenced primarily by the shape of the fault is almost totally overprinted by extreme local variations in the measured field. This made the transect difficult to use for modeling of the fault but did indicate large variations in magnetic susceptibility in both the ultramafic and volcanic/sedimentary units.

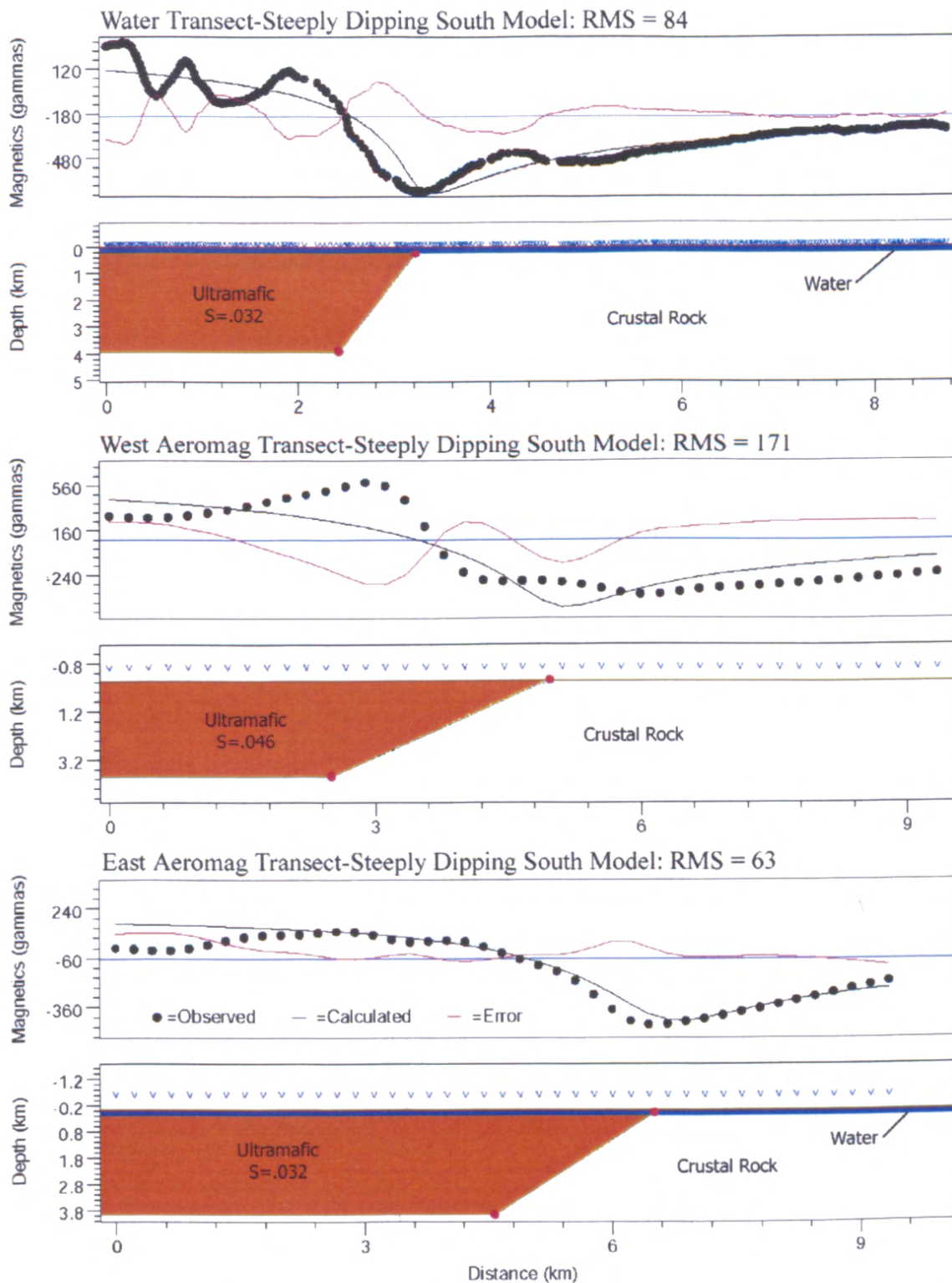


Figure 7a. South dipping high-angle fault models. RMS sum for this orientation is 318, the smallest misfit of the five orientations. Profiles are from south to north. "S" indicates susceptibilities, with values given in SI. Blue V's represent the locations at which measurements were taken.

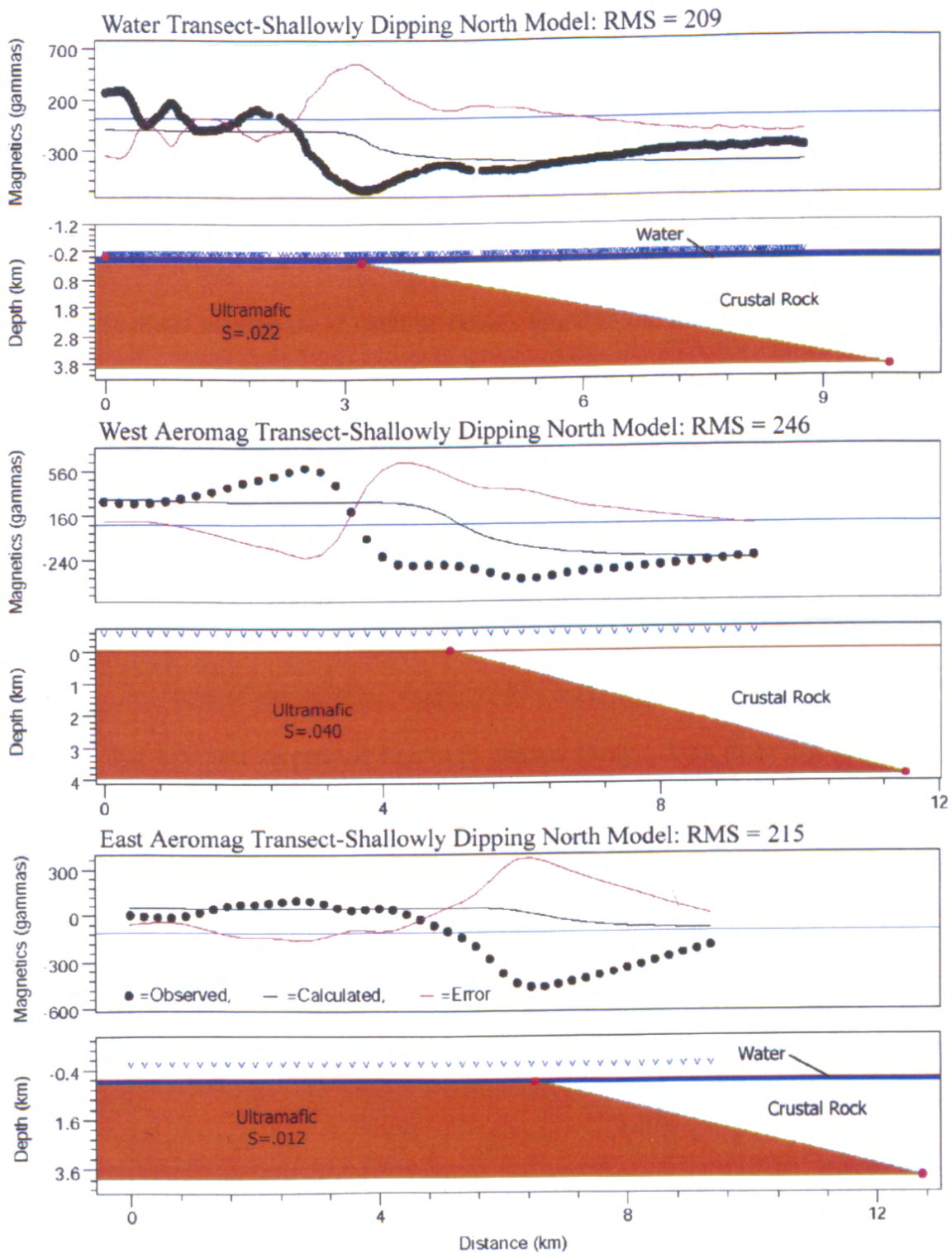


Figure 7b. North dipping low-angle fault models. RMS sum is 670, the highest misfit of the five orientations.

One interesting aspect of the ground-based data is the anomaly fluctuations in the volcanic and sedimentary unit of the Lummi Formation. Based on the measured susceptibilities of the basalts and other rocks in this middle section, this unit should have a relatively low anomaly profile compared to the ultramafics. The anomaly data actually show larger anomaly values in this unit than in the ultramafic unit (Fig. 8). The source of these fluctuations may be the serpentine bodies found in the midst of the middle section of the island. As mentioned, these are found throughout the volcanic/sedimentary unit and are of a soft, shiny, green appearance and texture representative of highly altered ultramafic rock. However, field observations do not show the volume of serpentine required to account for the extreme anomaly fluctuations. One aspect of serpentine that may help to explain this lack of prevalence is its highly unstable nature at the surface of the Earth. As much of the island is vegetated and many of the rocks highly weathered, it is likely that exposed serpentine has been eroded away. This does not preclude the possibility of large amounts of well distributed, subsurface serpentine.

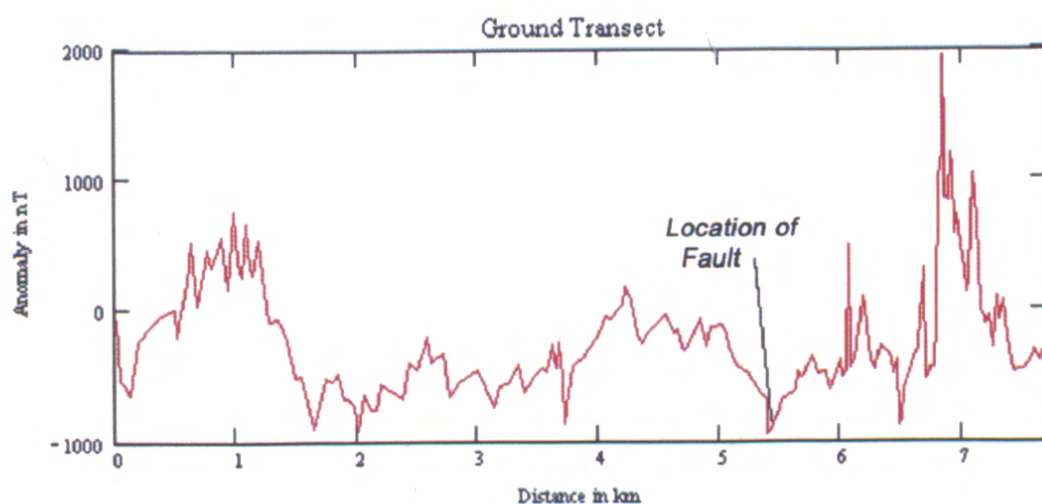


Figure 8. Ground transect with location of fault labeled. South is on the left. High frequency anomaly variations made this profile difficult to model, but did indicate unexpected, significant numbers of magnetic bodies in the basalt unit, north of the fault.

To examine this possibility, a model was prepared of the water transect with bodies of serpentine added. The air and water based transects show a fairly large amplitude anomaly increase over the volcanic/sedimentary unit (Fig. 9). By inserting serpentine bodies into the basalt unit, this increase can be accounted for. Additionally, the variance in the anomaly over the ultramafic unit can be accounted for by adding areas of differing susceptibility within it, representing differently altered sections of ultramafics to serpentine (Fig. 10). As an alternative possibility, models were also made using the small susceptibility values for the basalt gathered by Burmester et al. (2000). Magnetic basalt alone was unable to account for the observed anomalies.

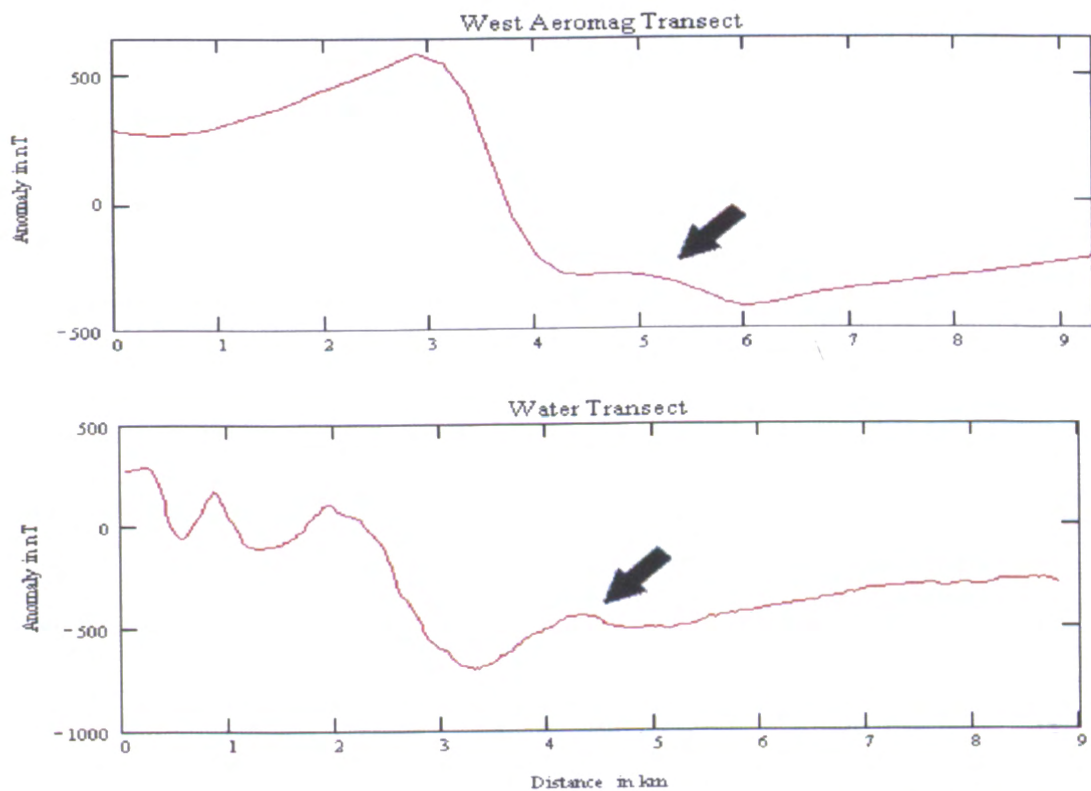


Figure 9. Anomaly increase over volcanic/sedimentary unit indicating the presence of significant amounts of magnetic material for the middle section of the island.

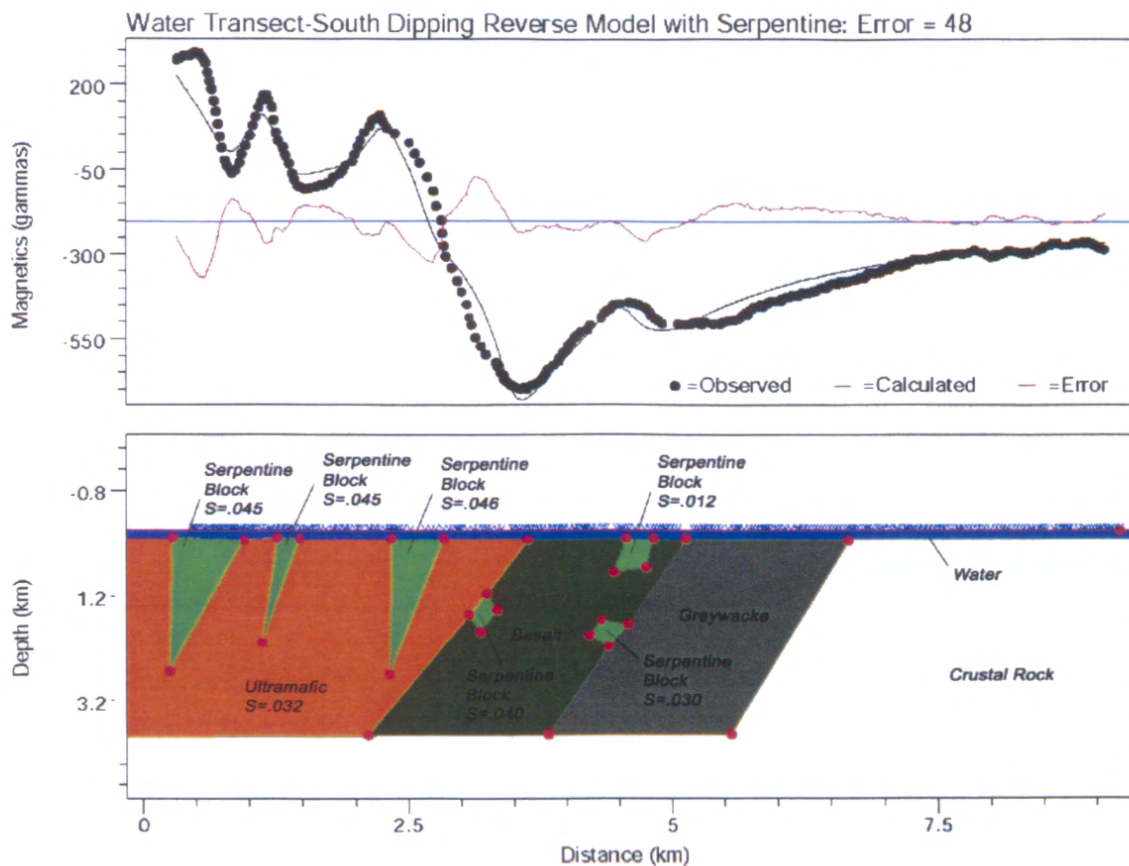


Figure 10. Model of water transect with high angle south dipping fault. Areas of differing amounts of serpentinization have been added to the ultramafics, and serpentine bodies have been added to the basalt (volcanic/sedimentary unit) to improve the fit of the model. South is on the left.

Discussion: The results of the modeling indicate that the fault is high-angle and south dipping with the ultramafics structurally above the volcanic/sedimentary unit. While the south dipping geometry was not unexpected, the high-angle aspect is. Many of the models for the geologic history of the San Juan Islands involve area-wide compression and thrusting (Brandon and Cowan 1985; Brown, 1987; Brandon et al., 1988; Maekawa and Brown, 1991). This type of movement is not generally associated with high angle faults (Twiss and Moores, 1992).

While it is feasible to have compressional displacement accommodated by creation of a high angle fault, it seems likely here that further explanation is necessary. Perhaps the initial creation of the fault was by tensional stress, making a high angle normal fault which later moved in a reverse manner to accommodate compressive stress. A second possibility is rotation of the fault from its created orientation to its present one. Also possible is that the fault is listric and becomes low-angle at depth. Limitations on modeling prevent the exclusion of this possibility. The simplest explanation is that it really is a normal fault. Whatever the model, within it the orientation of this fault requires justification.

A second unexpected finding was the extreme variation in susceptibility displayed by the ground surveys. The explanation for this variation in the anomaly for the ultramafics is supplied by what is known empirically, that local variations in serpentinization are present. Differences in degree of serpentinization lead to variations in susceptibility (Dunlop and Özdemir, 1997). These variations would both reinforce and subtract from each other magnetically thereby creating the observed anomaly. Variation in susceptibility for the ultramafics on a lower frequency than in the ground data can be seen in the water and air based data, and local variations of susceptibility were found in the samples taken by Burmester et al. (2000).

The volcanic/sedimentary unit, however, seems more complicated. Several facts need to be accounted for. First, like the ultramafics (only more so), there are extreme high frequency and amplitude variations in the measured anomaly (Figs. 8,9). Second, susceptibilities measured for the basalt and other rocks in the middle section of the island are not large enough to account for these variations. Third, highly magnetic serpentine,

along with a variety of non-magnetic rocks, are seen distributed throughout the volcanic/sedimentary unit. The final model of this study supports the idea of subsurface, well-distributed serpentine in the volcanic/sedimentary unit (Fig. 10). This accounts for the above facts, but does not explain why extensive serpentine would be present.

One possibility is that the volcanic/sedimentary unit is a serpentine melange. The definition of melange is broad and arguments over its true meaning exist, but generally they are zones containing many rock types of various sizes in some kind of matrix. One definition says they are “characterized both by the lack of internal continuity of contacts or strata and by the inclusion of fragments and blocks of all sizes, both exotic and native, embedded in a fragmented matrix of finer grained material,” (Raymond, 1975).

In the case of the volcanic/sedimentary unit of Cypress Island, the multitude of rock types and their distribution satisfies the block and fragment and lack of internal continuity criteria. The missing observable feature is the matrix. Serpentine is the proposed material here based on the measured subsurface extent of a highly magnetic material. Also, serpentine matrix melanges are a common result of tectonically and hydrothermally altered ophiolites, many of the components of which are present on Cypress Island (Saleeby, 1984).

At least two possible histories exist for this melange. The first is that the ultramafics that compose the matrix are different from the current ultramafic unit of the island. They would instead have been part of the ocean floor underlying the basalt of the volcanic/sedimentary unit (either the MORB or both the OIB and the MORB) (Fig. 2). Serpentinization of these ophiolite ultramafics would have begun almost as soon as they were formed and continued through subduction as the unit was sheared and mixed

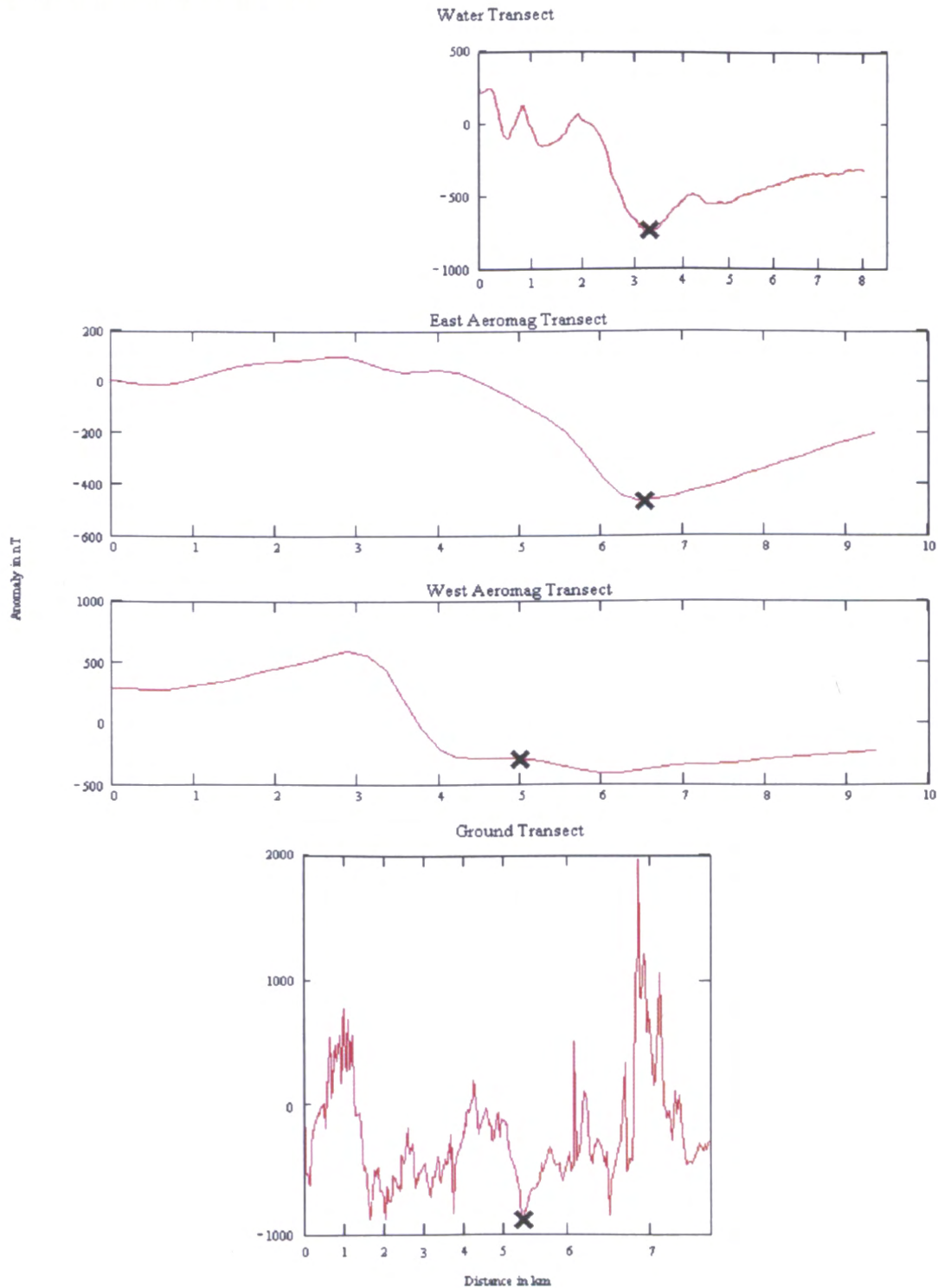
(Saleeby, 1984). After subduction, the already melanged unit could have been faulted to the surface and placed next to the unrelated ultramafic unit we see today.

A second possibility is that the Lummi Formation was subducted as a whole without underlying ultramafics, in the process creating fracturing and deformation. Then, as it was faulted to the surface the basalts were faulted as a unit between the already present greywackes and ultramafic rocks of the overriding continental plate or island arc (Fig. 2). This process would continue to fracture the basalts and add pieces of the greywacke and ultramafic units to them. This fractured body would be an excellent conduit of fluids and would allow serpentinization of the ultramafics included in it. As they serpentinized, their newly ductile nature would disperse them throughout the melange. This proposal is supported by the apparent cohesiveness of the greywackes to the north, which are less deformed than the basalts.

Several future studies could help resolve some of these issues. One way to narrow down the origin of the melange would be to examine the serpentine in it and find out if it was indeed the same as the ultramafic rocks making up the south part of the island. Also, knowing more about the greywackes would help to define the extent of the melange. The ground based transect did not cover these rocks, and according to the air and water based data, they are magnetically quiet. Discovering extensive serpentine in them as well would suggest that they too are a part of the melange. Finally, evidence to explain the orientation of the fault should be looked for. Indication of recent normal movement along the fault would add an interesting new element to the geologic history of the area.

Appendices

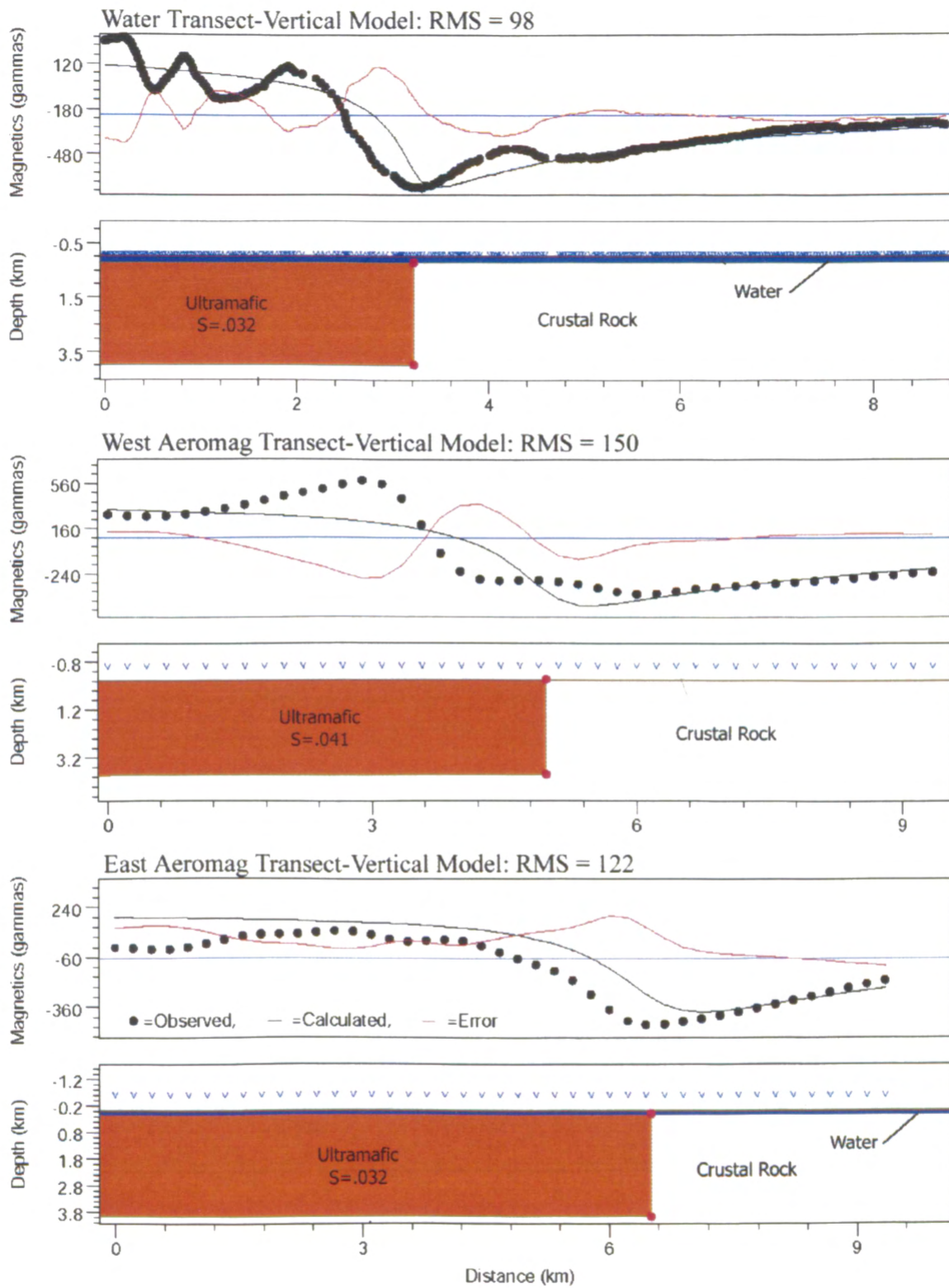
Appendix A: Comparison of four anomaly profiles used. Y-axis (anomaly) is scaled consistently for all four. X-axis (distance) scale is varied to display approximate locational relationship of the transects (Fig. 5). Beginning and end points for each are aligned by longitude. Fault locations are indicated by the black X's and are similarly aligned. South is on the left.



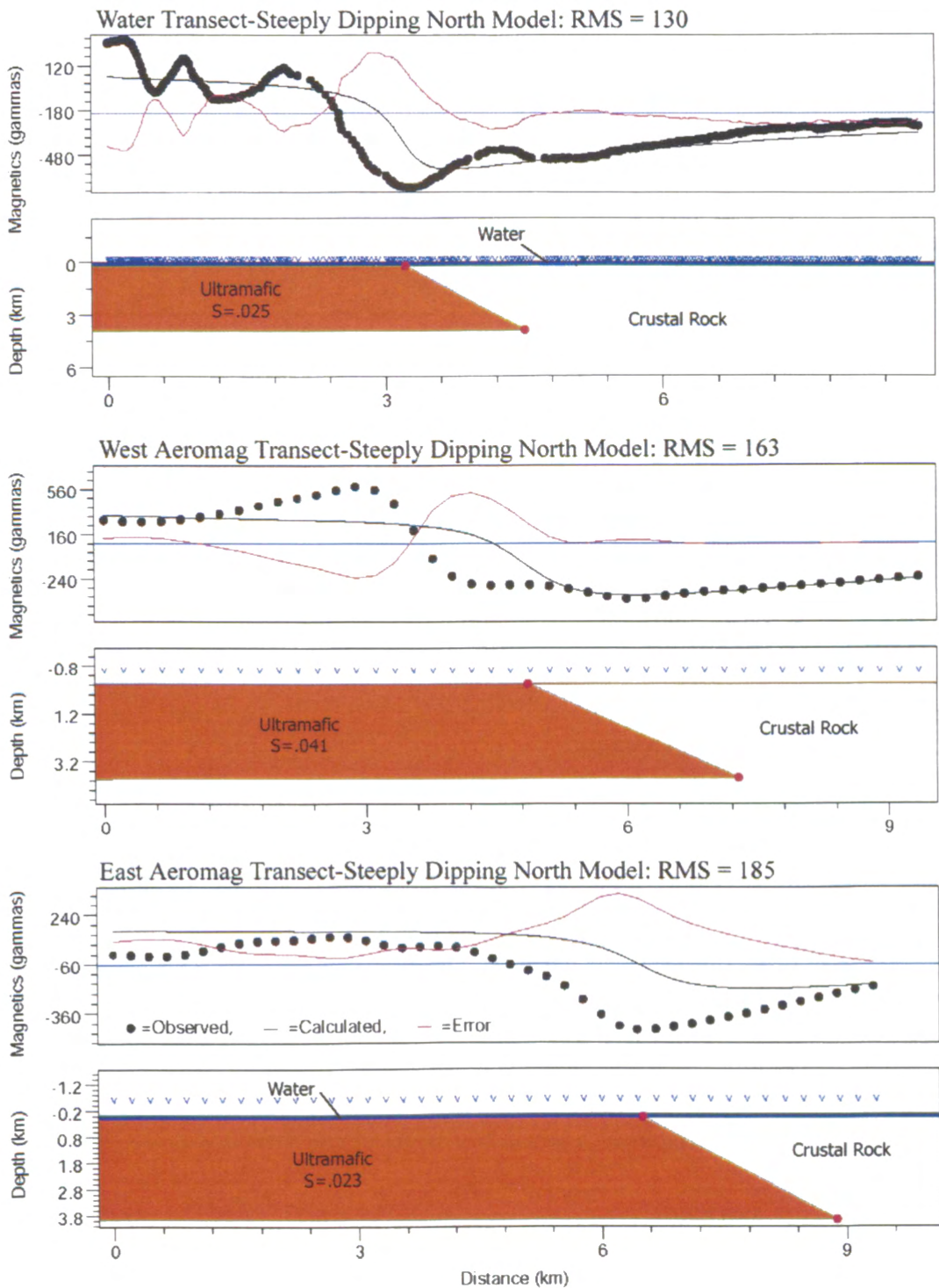
Appendix B: Measured susceptibility values for samples from Cypress Island taken by Burmester et al. (2000).

Ultramafic Susceptibilities (SI)	Mean		Volcanic/Sedimentary Susceptibilities	Mean
0.0191	0.0877		0.0065	0.0159
0.0584			0.0560	
0.0583	Median		0.0072	Median
0.0472	0.0522		0.0420	0.0080
0.0191			0.0080	
0.0261			0.0088	
0.0328			0.0078	
0.0452			0.0104	
0.0941			0.0030	
0.2080			0.0021	
0.0755			0.0065	
0.2633			0.0088	
0.1299			0.0067	
0.0397			0.0083	
0.0667			0.0055	
0.3349			0.0622	
0.1764			0.0202	
0.0434				
0.0393				
0.0522				
0.0121				

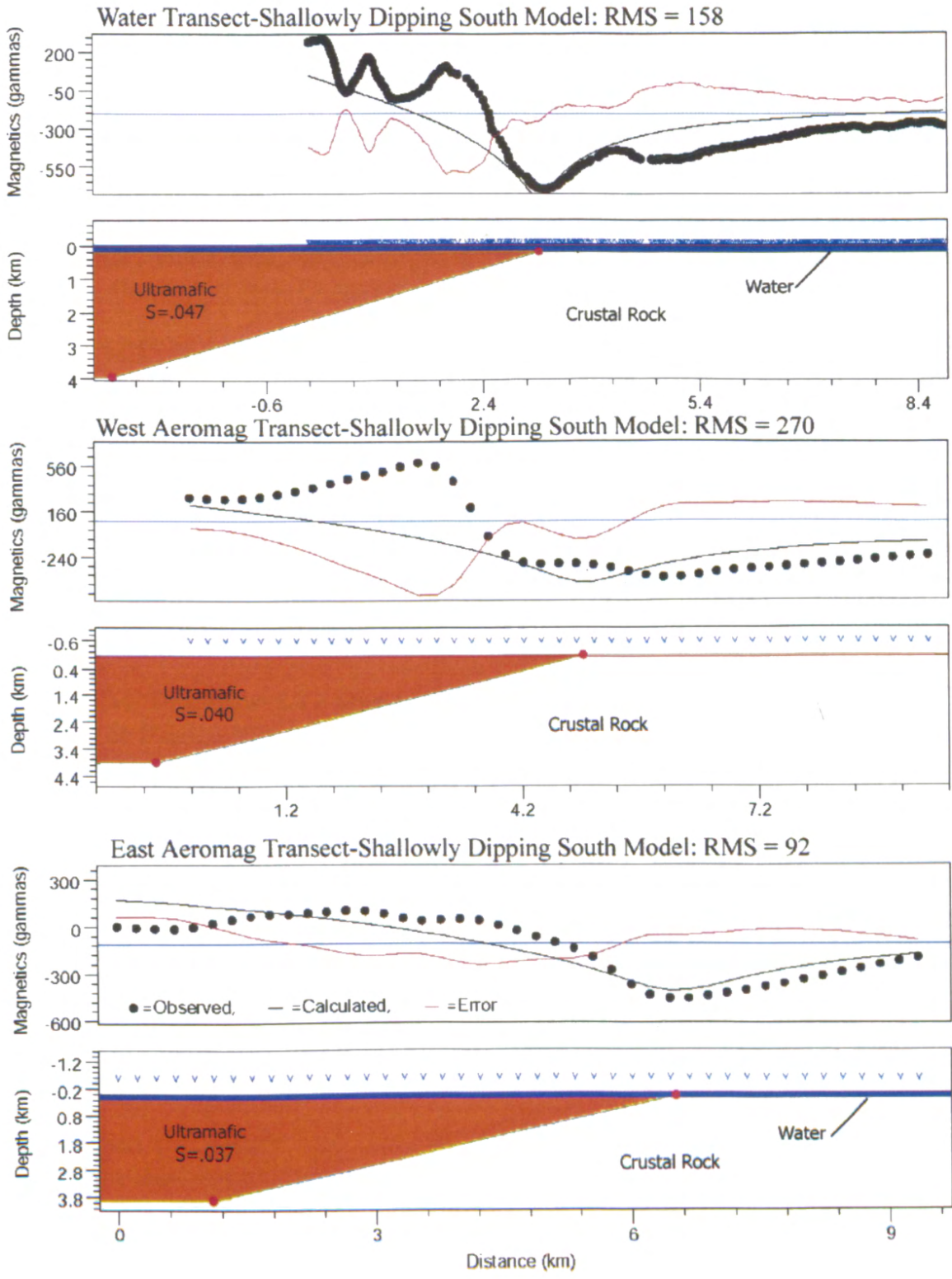
Appendix C.1- Vertical fault models. RMS sum is 370.



Appendix C.2- North dipping high-angle fault models. RMS sum is 478.



Appendix C.3- South dipping low-angle fault models. RMS sum is 520.



Acknowledgments and Thanks:

Dave Engebretson, George Mariz, Juliet Crider, Jack Mynatt, Liz Schermer, Travis Montgomery, Bernie Housen, Ben Stanton, Russ Burmester, Jeremy Davies, Lauren Kapp, Barbee Teasley and Abby Polus

References:

- Blake, M.C., Jr.; Burmester, R.F.; Engebretson, D.C.; Aitchison, Jonathon, 2000, Accreted terranes of the eastern San Juan Islands, Washington [abstract]: Geological Society of America Abstracts with Programs, v. 32 no. 6, p. A-4.
- Blakely, R.J., Wells, R.E., and Weaver, C.S., 1999, Puget Sound aeromagnetic maps and data, U.S. Geological Survey Open-File Report 99—514
- Brandon, M.T.; Cowen, D.S., 1985, The Late Cretaceous San Juan Islands-Northwestern Cascades thrust system [abstract]: Geological Society of America Abstracts with Programs, v. 17 no. 6, p. 343.
- Brandon, M.T.; Cowen, D.S.; Vance, J.A., 1988. The Late Cretaceous San Juan thrust System, San Juan Islands, Washington: Geological Society of America Special Paper 221
- Brown, E.H., 1987, Structural geology and accretionary history of the Northwest Cascades system, Washington and British Columbia: Geological Society of America Bulletin, v. 99, no. 2, p. 201-214.
- Brown, E.H.; Bradshaw, J.Y.; Mustoe, G.E., 1979, Plagiogranite and kyanophyre in ophiolite on Fidalgo Island, Washington: Geological Society of America Bulletin, v. 90, no. 5, p. 493-507
- Burmester, R.F.; Blake, M.C., Jr.; Engebretson, D.C., 2000, Remagnetization during Cretaceous normal superchron in eastern San Juan Islands, WA; implications for tectonic history: Tectonophysics, vol. 326, no.1-2, pp.73-92
- Carroll, P.R., 1980, Petrology and structure of the pre-Tertiary rocks of Lummi and Eliza Islands, Washington: University of Washington Master of Science thesis
- Dunlop, D.J.; Özdemir, Ö., 1997, Rock Magnetism: Fundamentals and Frontiers, Cambridge University Press
- Engebretson, D.C.; Blake, M.C., Jr., 2002, Alternatives to Mesozoic plate configurations and terrane displacements within the Pacific Basin and along western North America [abstract]: Geological Society of America Abstracts with Programs,
- GEOMAG, John M. Quinn, 2000; <http://geomag.usgs.gov/frames/geomagix.htm>
- GM-SYS Version 4.04, Northwest Geophysical Associates, Inc., 1998

Gussey, D.L., 1978, The geology of southwestern Fidalgo Island: Western Washington University Master of Science thesis

Hunt, C. P., Moskowitz, B. M., Banejee, S. K., 1995, Rock Physics and Phase Relations, A Handbook of Physical Constants: AGU Reference Shelf 3

Lapen, T.J., 2000. Geologic map of the Bellingham 1:100,000 quadrangle, Washington: Washington Division of Geology and Earth Resources

Maekawa, H.; Brown, E.H., 1991; Kinematic analysis of the San Juan thrust system, Washington: Geological Society of America Bulletin, v. 103, p. 1007-1016

McLellan, R.D., 1927, The geology of the San Juan Islands: Seattle, University of Washington Publication in Geology no. 2, 185 p.

Raleigh, C.B., 1965, Structure and petrology of an alpine peridotite on Cypress Island, Washington, U.S.A.: Contributions to Mineralogy and Petrology, V. 11, no. 7, p 719-741

Raymond, L.A., 1975, Tectonite and melange-A distinction: Geology, v. 3, p. 7-9

Saleeby, J.B., 1984, Tectonic significance of serpentine mobility and ophiolitic melange: Geological Society of America Special Paper 198, p. 153-168

Sterner, John, 1995, Washington State topographic map:
<http://access.wa.gov/government/images/wa.gif>

Twiss, R.J.; Moores E.M., 1992; Structural Geology, W.H. Freeman and Company

Vance, J.A., 1975, Bedrock Geology of San Juan County. *In* Russell, R.H., editor, Geology and water resources of the San Juan Islands, San Juan County, Washington: Washington Department of Ecology Water-Supply Bulletin 46, p. 3-19

Whetten, J.T., 1975, The geology of the southeastern San Juan Islands, *in* Russell, R.H., ed., Geology and water resources of the San Juan Islands: Washington Department of Ecology Water Supply Bulletin 46, p. 341-357